The mechanism of catalysis of the chorismate to prephenate reaction by the *Escherichia coli* mutase enzyme

Sun Hur and Thomas C. Bruice†

Department of Chemistry and Biochemistry, University of California, Santa Barbara, CA 93106

Contributed by Thomas C. Bruice, November 26, 2001

Molecular dynamics studies of the *Escherichia coli* chorismate mutase (EcCM), containing at the active site chorismate and in turn the transition state (TS), have been performed. The simulations show that TS is not bound any tighter than chorismate. Comparison of average polar interactions show they are virtually identical for interactions of EcCM with chorismate and the TS, whereas hydrophobic interactions with TS are much weaker than with chorismate. Interactions and the mechanism of catalysis of chorismate → prephenate by the EcCM enzyme are discussed.

Tighter binding of transition state (TS) as compared with substrate ground state (GS) is the most often used explanation for efficiency of enzymatic catalysis (1). We have initiated investigations of the dynamic structures of enzyme·ground state (E·GS) and E·TS to compare electrostatic and hydrophobic interactions of enzyme with GS and TS. Our goal has been to determine whether TS preferential binding over GS is (*i*) a tenet for all enzymes, (*ii*) always present but other things also contribute, or (*iii*) important in some enzymatic reactions but not in others. Theoretical arguments for the tenet that TS stabilization drives enzyme catalysis is based on Scheme 1. In this model, K_{TS}

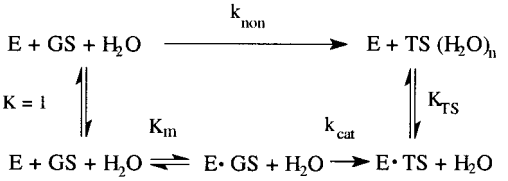

Scheme 1.

is the ratio of nonenzymatic reaction rate over enzymatic reaction rate $K_{TS} = k_{non}(K_m/k_{cat})$. The equilibrium constant for dissociation of E·TS in water is generally taken as K_{TS}. Observed from a different standpoint, Scheme 1 becomes Scheme 2 and

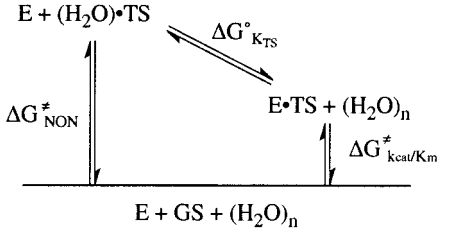

Scheme 2.

$\Delta G^\circ_{KTS} = \Delta G^{\neq}_{NON} - \Delta G^{\neq}_{kcat/Km}$. Thus, ΔG°_{KTS} is nothing more than a measure of the difference in free energies of activation for the enzymatic and nonenzymatic reaction, and this free-energy difference reflects all features of the enzymatic and nonenzymatic reactions. There is no theoretical reason to believe that K_{TS} reflects binding affinity of TS to enzyme. On the continuum of our study, we have chosen to examine a chorismate (CHOR) mutase. In this class of enzymes, there is no direct participation of enzyme in the chemical reaction (2–4) and TS geometry in an enzyme-catalyzed reaction is similar to TS in a noncatalyzed reaction (5, 6). These features enable us to directly compare the binding modes of enzyme with TS and GS (7).

CHOR mutases increase the rate of the Claisen rearrangement of CHOR to prephenate (Scheme 3) by greater than 10^6-fold

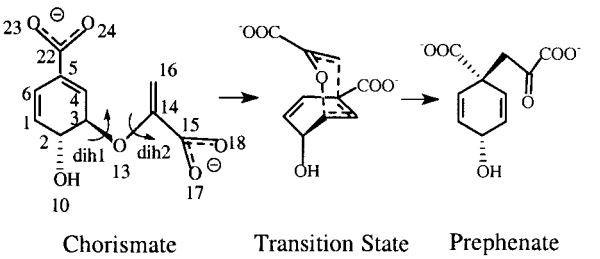

Scheme 3.

relative to the reaction in water (8). The crystal structures of CHOR mutase from *Bacillus subtilis* (BsCM) (4), *Escherichia coli* (EcCM) (9), and yeast (10) have been solved. The majority of studies on CHOR mutase have focused on BsCM.

A hydrogen bond between a negatively charged glutamate and the hydroxyl group of CHOR is critical to the reaction in BsCM (11) but not in EcCM. There is only one arginine holding the carboxylate at the side chain of CHOR in BsCM, whereas both carboxylates of CHOR are strongly held by two arginines in EcCM. The extensive exposure to the solvent and versatile mode of hydrogen bonds observed in the active site of BsCM show a great counterpoint to the extremely stable hydrogen bonding network observed in the EcCM active site. The active site of EcCM is buried in the protein and allows little solvent accessibility. The BsCM catalyzed reaction is slowed when solvent viscosity is increased, whereas the EcCM catalyzed reaction is not (12). For BsCM, kinetic isotope-effect experiments show the rate-determining step is largely in the chemical rearrangement (13), whereas in EcCM it is not so under the same V_{max}/K_m condition (14). The two enzymes differ in structures of E·CHOR complex and kinetic handling of the pericyclic rearrangement.

Abbreviations: CHOR, chorismate; TS, transition state; GS, ground state; TSA, endo-oxabicyclic transition state analogue; EcCM, monofunctional CHOR mutase from *E. coli*; BsCM, CHOR mutase from *B. subtilis*; NAC, near attack conformer; MD, molecular dynamics.

†To whom reprint requests should be addressed. E-mail: tcbruice@bioorganic.ucsb.edu.

The publication costs of this article were defrayed in part by page charge payment. This article must therefore be hereby marked "*advertisement*" in accordance with 18 U.S.C. §1734 solely to indicate this fact.

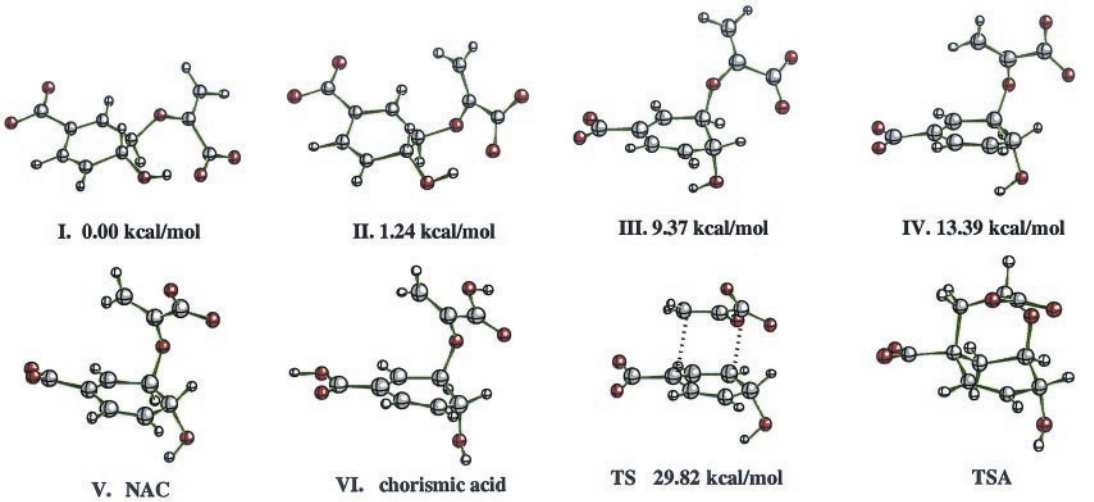

Fig. 1. Conformers and structures.

Although the rate constants for the catalysis are much the same among these enzymes, the enthalpy and entropy components of the free energies of activation are very different. For the uncatalyzed reaction in water, $\Delta H^{\neq} = 20.5$ kcal/mol and $-T\Delta S^{\neq} = 3.9$ kcal/mol. These become 12.7($\Delta H^{\neq}$), 2.7($-T\Delta S^{\neq}$), in the BsCM-catalyzed reaction, and 16.3($\Delta H^{\neq}$), 0.9($-T\Delta S^{\neq}$) in the EcCM-catalyzed reaction. This compensation between $\Delta H^{\neq}$ and $T\Delta S^{\neq}$ reflects the differences in mechanism.

In this article, we report two 2.1-ns molecular dynamics (MD) simulations of EcCM complexed in turn with CHOR and the TS in both active sites. We find that the TS is not bound more tightly than the substrate. Instead, the active site confines the reacting C5-C16 centers of CHOR into a very close proximity. This geometrical compression is accomplished by restriction of substrate space rather than GS strain.

Methods

Optimization of CHOR Conformers. The CHOR conformers, TS, and chorismic acid conformer (Fig. 1) were located at the MP2/aug-cc-pVDZ//B3LYP/6–31 + G(d,p) level of theory by using GAUSSIAN98. The initial TS structure was that calculated by Houk and Wiest (15) and confirmed by a single negative frequency at the HF/6-31G(d) basis set level.

MD Simulations. Among the four conformers of chorismate (Fig. 1) the one which most resembles the TS structure is conformer IV with the highest energy. This conformer IV and TS were docked to the active site of the crystal structure of EcCM·TSA (Protein Data Bank ID Code 1ECM) (9) by replacing endo-oxabicyclic transition-state analog (TSA) with CHOR(IV) or TS. The program CHARMM V 25b2 was used for the simulations. To maintain the geometry of allyl vinyl moiety of TS, high force constants were used for forming-bond (C5-C16), breaking-bond (C3-O13), and any angle that involved the two bonds. The system was placed into a rectangular box of water to use a periodic boundary condition and was energy-minimized before the simulation began. Details of the methods for parametrization and simulation are provided in *Supporting Methods*, which is published as supporting information on the PNAS web site, www.pnas.org.

Results

Each of the two active sites of EcCM is formed by 3 helices from one subunit and a helix from the other subunit. A residue with an asterisk (i.e., Arg-11*) denotes a residue in the single helix from the other subunit. The distance between ATOM1 of a protein residue and ATOM2 of a ligand will be denoted as residue(ATOM1)-ATOM2 [i.e., Gln-88(OE1)-O13]. When both atoms forming the distance are of a same ligand, only atom names will be designated (i.e., C5-C16).

Positional Fluctuations. The positional fluctuations of the CA and CHOR/TS were calculated. Much of the enzyme exhibits similar flexibility in EcCM·CHOR and in EcCM·TS, but the loop near the active site (residues 42–48) shows higher fluctuation in EcCM·TS than in EcCM·CHOR by ≈0.3 Å. The fluctuation of CHOR is similar to that of TS (≈0.5 Å) except for the moiety that is fixed by high force constant to maintain the TS geometry (Fig. 2).

Interaction Between EcCM and Both CHOR and TS. In Fig. 3 we divided the interactions between EcCM and CHOR or TS into electrostatic interactions and hydrophobic interactions. Residues that are involved in electrostatic interactions are Arg-11* salt-bridged to the carboxylate of the side chain (C15), Arg-28/Ser-84 salt-bridged/hydrogen-bonded to the ring carboxylate (C22), Gln-88/Lys-39 hydrogen-bonded to the ether oxygen (O13), and Asp-48 hydrogen-bonded to the hydroxyl group (O10). The interaction distances between EcCM and ligand (CHOR or TS) and between EcCM residues are summarized in Tables 2 and 3, which are published as supporting information on the PNAS web site. To avoid confusion, only active site (B), which is surrounded by 3 helices from subunit (B), will be discussed. Most of the features are similarly observed in active site (A) when comparing EcCM·CHOR(A) and EcCM·TS(A).

The distances of electrostatic bonding of two carboxylates of CHOR with Arg-11* and Arg-28 are similar to the distances for TS bonding. Both CHOR and TS distances are shorter than the crystallographic values with TSA. The relative positions of Arg-11* and Arg-28 are very well matched in EcCM·CHOR and

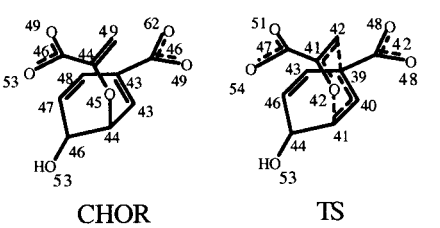

Fig. 2. Positional fluctuations (X10^{-2}Å) of each heavy atom of ligands bound to the active site of EcCM.

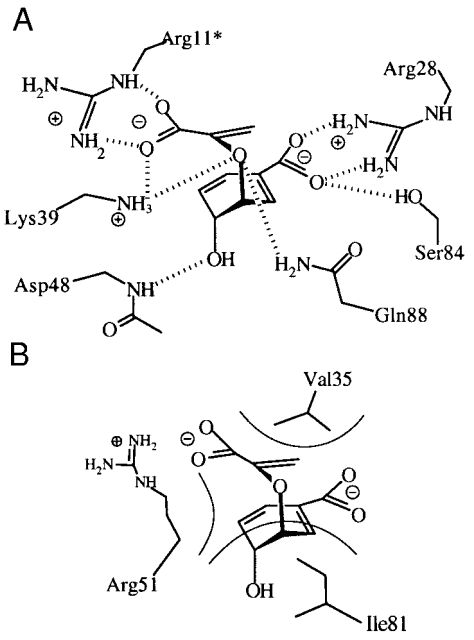

Fig. 3. (*A*) Electrostatic interaction. (*B*) Hydrophobic interaction.

EcCM·TS. The immobility of the guanidino groups of Arg-11* and Arg-28 results from auxiliary residues, mechanically fixing the position of the guanidino groups (Fig. 4). Arg-11* is stacked between Arg-51 and Leu-7* and forms a salt bridge with Asp-48. The guanidino group of Arg-28 is fixed by a salt bridge with Asp-18* and van der Waals contact with Ile-80. Thus, the two major functional groups used in binding of CHOR, i.e., guanidino groups of Arg-11* and Arg-28, are rigidly preorganized, resulting in the distance between the enzyme bound CHOR carboxylates (C15-C22) being 5.50 ± 0.23 Å in EcCM·CHOR, whereas C15-C22 of the conformer IV is 6.49 Å. For TS, C15-C22 is 5.14 ± 0.08 Å in the active site and 5.19 Å in the gas phase.

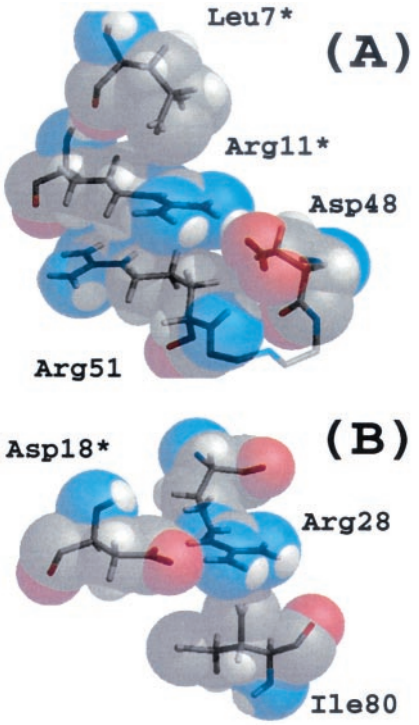

Fig. 4. (*A*) Auxiliary residues supporting Arg-11*; Arg-51, Leu-7*, and Asp-48 fix the position of the guanidino group of Arg11*. (*B*) Auxiliary residues supporting Arg-28; Asp-18* and Ile-80 fix the position of the guanidino group of Arg-28.

Gln-88(NE2) and protonated Lys-39(NZ) are hydrogen-bonded to O13 of both CHOR and TS. The distance between Gln-88(NE2) and O13 of EcCM·CHOR is similar to that of EcCM·TS, whereas Lys-39(NZ)-O13 in EcCM·CHOR is longer than in EcCM·TS by ≈0.2 Å. However, because of the hydrogen bond between Lys-39(NZ) and Gln-88(OE1), the closer Lys-39(NZ)-O13 in EcCM·TS induces a shorter distance between the two negatively charged oxygen Gln(OE1) and O13 by the same amount (≈0.2 Å). The Lys-39 makes another salt bridge with carboxylate O17 of CHOR and TS. The distance between Lys-39(NZ) and O17 is longer in EcCM·TS than in EcCM·CHOR by 0.07 Å. The Lys-39 is free to rotate around Lys-39(NZ) in EcCM·TS active sites; however, in EcCM·CHOR it is not. This finding suggests that the specific hydrogen bonds between Lys-39 with CHOR are lost in EcCM·TS.

In the crystal structure of EcCM·TSA, two hydrogen bonds are formed between the hydroxyl group of TSA and Glu-52 and Asp-48 in EcCM. In our simulation, only one hydrogen bond was found between hydroxyl O10 and Asp-48(HN), and this hydrogen bond is similar in length in EcCM·CHOR and EcCM·TS. The hydrogen bonds between the carboxylate Glu-52(OE2) and O10 of either CHOR or TS were present in the initial coordinates (energy minimized structure) but disappeared in all active sites when the structures were taken to ambient temperature before MD simulation. The average distance between Glu-52(OE2) and O10 becomes greater than ≈5 Å. Instead of making a hydrogen bond to CHOR and TS, Glu-52 forms a salt bridge with Arg-47.

In comparing EcCM·CHOR and EcCM·TS, the difference in the interacting distances between EcCM and CHOR or TS is less than 0.3 Å. However, the differences in hydrophobic interactions are 0.5–1 Å. Those residues involved in hydrophobic interactions are Val-35 (in van der Waals contact with C16), Ile-81 (in contact with C5), and Arg-51 (in contact with C1) (Fig. 3*B*). All of the van der Waals contacts between CHOR and EcCM are absent in the EcCM·TS. The TS is not as closely associated with the enzyme as is CHOR (Fig. 5)!

C16, one of two reactive components of CHOR, makes a van der Waals contact with Val-35, which is released on contraction of the C5–C16 distance to form the TS. The distance between Val-35(CG1) and C16 is 3.65 (EcCM·CHOR) < 4.06 (EcCM·TS) < 4.92 Å (EcCM·TSA). This order is the reverse order of the C5–C16 distance; 1.54 (EcCM·TSA) < 2.58 (EcCM·TS) < 3.48 Å (EcCM·CHOR).

C5, the other reactive component of CHOR, makes a close contact with Ile-81 in EcCM·CHOR. The average Ile-81(CD)-C5 is 3.83 Å and it reached ≈3.6 Å when C5-C16 reached ≈3.2 Å. However, this contact was not found in EcCM·TS. The difference comes from the conformation of Ile-81. The dihedral angle formed by C-CA-CB-CG1 of Ile-81 in EcCM·CHOR is twisted such that CD of Ile-81 orients toward C5 of CHOR, whereas CG2 of Ile-81 points toward C5 of TS. Because of the lack of an additional methyl group at CG2, contact between C5 of CHOR and Ile-81 is absent in EcCM·TS.

The change in the position of Arg-51 is rather drastic when EcCM·CHOR is converted to EcCM·TS. As depicted in Fig. 5, Arg-51 intervenes between the ring and the side chain of CHOR. This structural feature is not found in EcCM·TS, because of the small space between the ring and the side chain of TS. As a result, Arg-51 moves away on formation of TS. As a measure of the relative position of Arg-51, the distance between Arg-51(CG) and C1 and the angle formed by Arg-51(CG)-C3-C1 are compared in Fig. 5. In EcCM·CHOR, Arg-51(CG)-C1 is ≈0.5 Å

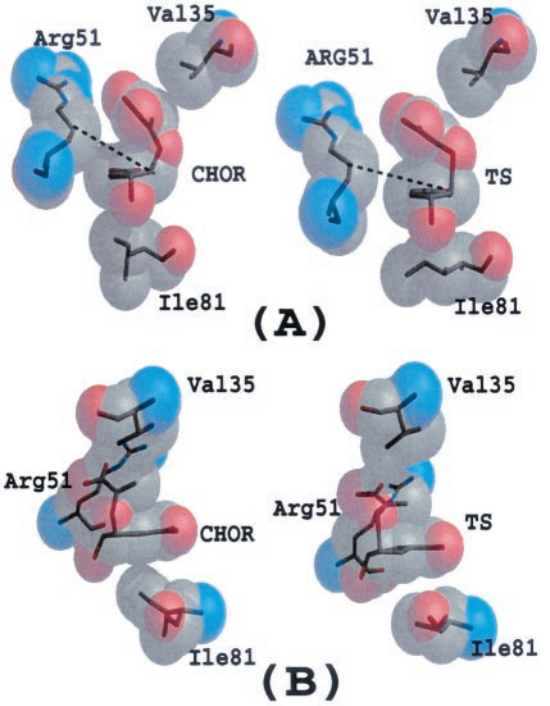

Fig. 5. Comparison of hydrophobic interactions in the EcCM·CHOR active site and the EcCM·TS active site. *A* shows the front view and *B* shows the side view of the averaged structure. CHOR has more van der Waals contacts with the enzyme active site than TS. The angle between the dotted line [Arg-51(CG)-C3] and the ring was used to measure the different position of Arg-51 relative to CHOR.

shorter than in EcCM·TS. The angle of Arg-51(CG)-C3-C1 is 33° in EcCM·CHOR, whereas the angle is 17° in EcCM·TS. The positional change of Arg-51 brings about several changes in the interactions between enzyme residues. The contact area between Arg-51 and Arg-11* is smaller in EcCM·TS than EcCM·CHOR. The hydrogen bond between Ser-15* and the guanidino group of Arg-51 in EcCM·CHOR is not present in EcCM·TS. The hydrogen bond between Arg-51(N) and Asp-48(O) in EcCM·CHOR is changed into the interaction with OD1 of Asp-48 in EcCM·TS (see *Supporting Methods*).

Conformational Analysis of CHOR in the Active Sites. After docking of CHOR conformer IV into the enzyme active site, there follows a side chain rotation by 10–20° around dih1 and dih2 (Scheme 2). As a result, CHOR in EcCM·CHOR resembles the TS structure more than does IV. This conformer is a reactive conformer [near attack conformer (NAC)] in respect that the bond-forming distance (C5-C16) and the angle at which C16 approaches C5 (i.e., attacking angle defined in Fig. 6) are in place to enter the TS. The averaged C5-C16 of CHOR is shorter than in IV by 0.3 Å, and the averaged attacking angle is smaller than in IV by ≈3° in CHOR. With the definition of NAC, the C5–C16 distance is shorter than the van der Waals interaction distance between vinyl carbons [3.7 Å (16)], and the attacking angle is less than 40°; ≈70% of conformers of CHOR are NACs (Fig. 7).

Discussion

Binding of CHOR and TS in the Active Site of EcCM. K_{TS} [$= k_{non}(K_m/k_{cat})$] was evaluated to be 2×10^{-5} (μM), whereas K_m is 40 (μM). Because the CHOR mutase reaction does not involve any covalent bond between the enzyme and the substrate or the TS, K_{TS}/K_m can be used to test the validity of the position that TS binding over GS binding determines enzyme efficiency. From

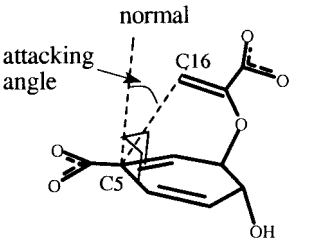

Fig. 6. Structural definition of NAC for the chorismate to prephenate reaction.

the results of our MD simulations, such tighter binding of the TS compared with CHOR was not observed.

The electrostatic interactions (Fig. 3*A*) between the residues of EcCM with CHOR or TS are virtually identical. The distances between the guanidino groups of Arg-28 and Arg-11* to the carboxylates of CHOR and TS are indistinguishable. This finding is not surprising between ionic interactions but the same behavior is also seen for the dipolar interactions. The interaction distance differs by less than <0.05 Å or changes into another interaction, which sums up to similar binding affinity.

A critical role of hydrogen bonding between Gln-88 and the ether oxygen (O13) of CHOR has been proposed based on mutational studies with EcCM (17). From our study, this hydrogen bond is of equal length in EcCM·CHOR and EcCM·TS. There still exists a possibility of stronger interaction between Gln-88 and O13 in the TS, if a negative charge develops on O13 on TS formation as proposed (17). The proposal does not seem to be so. The restrained electrostatic potential (RESP) charges at O13 in CHOR and TS are −0.415 and −0.419 a.u., respectively. This insensitivity in the charge of the ether oxygen on going from CHOR to the TS has also been reported (18, 19). In the study by Worthington *et al.* (19), it was also shown that preferential stabilization of the TS ether oxygen by forming the hydrogen bond is insignificant. The 1,000-fold drop of k_{cat}/K_m in mutant Gln-88Glu relative to the wild-type enzyme can be explained in terms of substrate binding (K_m) rather than k_{cat} (17). After substituting the ether oxygen by CH_2 in the TSA, K_i has increased by 250-fold in separate substrate analogue experiments (20).

The hydrogen bond between protonated Lys-39 and O13 is shorter in EcCM·TS than EcCM·CHOR by ≈0.2 Å. However, this accompanies several unfavorable interactions between EcCM and TS. The repulsive force between ether oxygen of CHOR and Gln-88(OE1) increases, and the hydrogen bond between carboxylate(O17) of CHOR and Lys-39 becomes weaker in EcCM·TS. Thus, TS stabilization by Lys-39 interaction

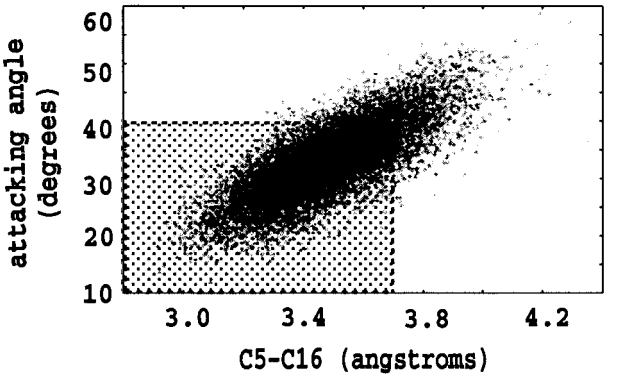

Fig. 7. Distribution of conformers along the C5 to C16 distance vs. the attacking angle (Fig. 6) in the active site of EcCM. Within the box (dotted region) conformers are defined as NAC. The mole fraction of NAC is ≈70%.

BIOCHEMISTRY

with O13 is, in balance, insignificant. The importance of Lys-39 seems to be in stabilizing the active site structure. All of the Lys-39 mutants show different circular dichroism spectra than wild-type enzyme, indicating that the enzyme structure changes when mutating Lys-39 (17). It is observed in our simulations that Lys-39 is hydrogen-bonded to four entities: O13 and O17 of ligand, OE1 of Gln-88, and O of Pro-46. When comparing each of the four interaction distances in EcCM·CHOR and EcCM·TS, the overall active site would seem to be more stable in EcCM·CHOR than in EcCM·TS. This idea is supported by the observation that the loop structure at residues 42–48 fluctuates more in EcCM·TS than in EcCM·CHOR.

The changes in hydrophobic interactions on conversion of EcCM·CHOR to EcCM·TS are greater than are the changes in electrostatic interactions. The three van der Waals contacts of CHOR with Val-35, Ile-81, and Arg-51 are completely lost in EcCM·TS (Fig. 5). The positions of Val-35 and Ile-81, which form van der Waals contacts with two reactive termini (C16 and C5, respectively), do not change when going from EcCM·CHOR to EcCM·TS. The release of these hydrophobic interactions comes from the shorter distance between C5 and C16 in the TS structure relative to CHOR. The ≈1 Å shift of the hydrophobic chain of Arg-51 away from the active site, on going from less polar CHOR to polar TS, makes several protein residue–residue interactions less stable. The smaller contact area of Arg-51 with Arg-11* implies less favorable stacking (Fig. 4*A*). The change in the turn structure formed by Arg-51 and Asp-48 (discussed in *Results*) causes the hydrogen bond between Arg-11* and Asp-48 to break. In addition, the hydrogen bond between the guanidino group of Arg-51 and Ser-15* is broken in EcCM·TS. The complete loss of several hydrogen bonds between enzyme residues in the active site and the disappearance of van der Waals interactions between EcCM and the TS when EcCM·CHOR → EcCM·TS do not support the contention that TS stabilization is a driving force in the enzymatic catalysis.

Most importantly, the positional fluctuations calculated for CHOR and TS (Fig. 2) are similar in the nanosecond time range, indicating that the active site of EcCM is not restricting the motion of the TS more than for CHOR.

Glu-52. The absence of a hydrogen bond between the hydroxyl hydrogen of CHOR and Glu-52 in our simulation and its presence in the crystal structure needs careful consideration. Instead of forming the hydrogen bond with ligand, Glu-52 forms salt bridges with Arg-47 in both active sites of EcCM·TS and EcCM·CHOR. Considering that Glu-52 resides at the surface of EcCM, the hydrogen bond found in the crystal structure may be the result of the stabilizing effect from crystal lattice force. Glu-52 is inferenced to be important because of the parallel position of Glu-78 in BsCM, which is experimentally shown to be important for a BsCM-catalyzed reaction. However, few experiments show that Glu-52 is critical for EcCM catalysis. Kinetic experiments with substrates lacking the hydroxyl hydrogen (21) show 3% activity of the CHOR in EcCM reaction. The Glu52Gln mutation results in only a 3-fold decrease in k_{cat}. Interestingly, the same mutation in BsCM (Glu78Gln) results in the enzyme having <0.05% the specific activity of the wild type (11).

Reactive Conformers of Enzyme·Substrate (NAC). In general, the shape and charge distribution of enzyme active sites and placement of required functional groups encourages the formation of substrate conformers that closely resemble the TS (NAC). NAC formation is required before TS formation and is a key element in enzyme catalysis (7). In our simulation, NAC structures account for ≈70% of GS conformers. Thus, EcCM is very proficient to form NAC. The following two steps are proposed to be used by EcCM in NAC formation: (*i*, formation of PreNAC) When binding the two carboxylates of CHOR to solidly placed guanidino groups of two arginines, C16 of CHOR is placed under the CG1 of Val-35. This is accomplished by a rotation of the side chain of CHOR (dih1 and dih2) by 10–20° relative to conformer IV. (*ii*, formation of NAC) Val-35 reduces the conformation space of C16, resulting in a high population of conformers with two reactive termini (i.e., C5 and C16) in proximity.

Table 1. Average geometry of CHOR in EcCM active site and Ab initio-optimized geometries of CHOR(IV), chorismic acid (VI), and TS in the gas phase

Geometrical parameters	CHOR	CHOR IV	Chorismic acid VI	TS
C5–C16, Å	3.48 ± 0.19	3.78	3.65	2.58
Attacking angle, °	32.9 ± 6.0	35.6	43.47	8.10
dih1, °	62.2 ± 7.1	72.8	55.35	56.5
dih2, °	−91.8 ± 0.66	−77.3	−92.06	−72.5

Arg-11* and Arg-28. After binding of CHOR to the EcCM active site, the side chain is rotated by 10–20° from IV and conformer V is formed. This 10–20° rotation of the side chain along the C3-O13 and O13-C14 bond results from the constraint on the distance between the two carboxylates (C15-C22), which is imposed by the fixed distance between the guanidino groups of Arg-11* and Arg-28. However, this rotation of the side chain is at little cost in energy. The penalty in energy accompanying the rotation of the dih1 and the dih2 by 10–20° relative to IV is less than 2 kcal/mol for CHOR in the gas phase (at the MP2/aug-cc-pVDZ level of theory). This penalty is largely compensated in the energy by salt bridges formed between CHOR carboxylates and the two guanidino groups of arginines, which results in electrostatic stabilization. Furthermore, the conformation of enzyme-bound CHOR resembles the conformer of neutral chorismic acid (VI) in the gas phase (Table 1), that preorganization of the enzyme has the hydrogen bond donors (i.e., guanidino groups) in such a position that the "PreNAC" is formed in the most economic way without a strain.

The role of Arg-11* and Arg-28 in forming PreNAC is not restricted to conformer IV. More abundant conformer II also can bind and can be converted to PreNAC by Arg-11* and Arg-28. This finding has been recently shown for the CHOR

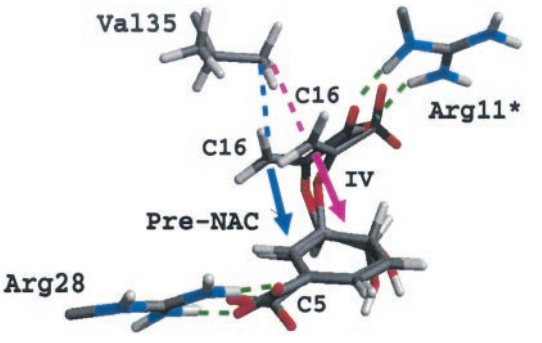

Fig. 8. Comparison of PreNAC and IV structure in the EcCM active site. Gas phase conformer IV is overlaid onto PreNAC structure in the active site. Without rotating dih1 and dih2 by 10–20° from IV geometry, C16 of IV is not tucked under Val-35 so that van der Waals contact of C16 with Val-35 can contribute to reducing the C5-C16 distance. Pink arrow from Val-35 to C16 points toward a different direction other than pointing toward C5. After the formation of PreNAC, Val-35, C16, and C5 become aligned (i.e., blue dotted line and blue arrow are aligned). Thus, the formation of PreNAC by two salt bridges between two carboxylates and Arg-11*/Arg-28 (green dotted lines) are prerequisite for formation of NAC.

mutase from yeast (22). Based on this study, we have docked conformer II into the active site of EcCM and energy-minimized the EcCM·CHOR complex. The initial conformer II becomes PreNAC after the minimization, by the change in the ring conformation from diequatorial to diaxial and by turning the side chain from the structure of II (5–10° in dih1 and 15–20° in dih2). The conversion from diequatorial to diaxial is brought about by the side-chain carboxylate forming an intermolecular hydrogen bond with Arg-11* at the expense of the intramolecular hydrogen bond with the hydroxyl group. The binding of the more prevalent conformer II to EcCM and further transformation into PreNAC (or NAC) is in good agreement with experimental results. A secondary kinetic isotope effect was not observed for the V_{max}/K_m condition with EcCM, which implies a slow step before the chemical rearrangement (14).

It has been suggested that stabilization of TS occurs on forming the salt bridges between the two carboxylates and Arg-11* and Arg-28. This claim is based on the idea that the repulsive force between two carboxylates is stronger in TS than in CHOR because of the shorter distance between them (15, 23) and that Arg-11* and Arg-28 remove this portion of the activation barrier. However, the proposed stabilizing effect of enzyme on TS must be compared with the reaction in water to explain the rate enhancement on going from water to enzyme. The study of the transferred nuclear Overhauser effects on CHOR (24) show that there is a conformer present in solution, in which the two carboxylates of CHOR are placed in proximity. This finding suggests that the negative charges of the carboxylates are sufficiently shielded in water. Thus, charge neutralization of CHOR, *per se*, in the EcCM active site cannot provide significant lowering of $\Delta H^{\neq}$ compared with the reaction in water.

Val-35. After rotation by 10–20° of the side chain of CHOR on binding to two guanidino groups of arginines, C16 is tucked under Val-35 (Fig. 8). The formed van der Waals contact between Val-35 and C16 (≈3.65 Å) efficiently restricts the space between two reactive termini (C5 and C16) (PreNAC → NAC).

Does Val-35 define the edge of a "box" that encompasses the substrate with close approximation of C5-C16? Or, does Val-35 push such that C5 and C16 are mechanically moved together in the TS? GS approximation or TS squeezing? To answer these questions, the correlation between the bond-forming distance (C5-C16) and "pushing distance " [Val-35(CG1)-C16] was investigated by plotting one distance vs. the other for all of the conformers from MD trajectories (Fig. 9). The round shape of the distribution shows that there is no correlation between the two distances. The shortest C5-C16 is achieved even though CG1 of Val-35 is not closest to C16 of CHOR. The lack of correlation between the C5-C16 and Val-35(CG1)-C16 rules out a mechanism in which Val-35 directly pushes C16 toward C5. By restricting the allowed maximum value of C5-C16, Val-35 just increases the NAC population without a strong strain.

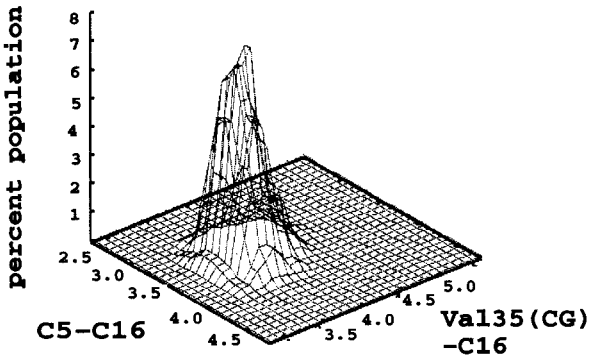

Fig. 9. Percent population of conformers as a function of C5 to C16 distance and Val-35(CG1) to C16 distance in EcCM·CHOR.

Conclusions

From the highly polar TS structure and the electrostatic interactions observed in the crystal structure of EcCM complexed with the TSA, it has been proposed that tighter binding of TS compared with substrate (CHOR) by EcCM is responsible for the $>10^6$ catalytic enhancement (8, 20, 25–27). The 100-fold tighter binding ($K_i/K_m = 100$) of TSA compared with CHOR has been interpreted as being caused by TSA being a transition state analogue. However, TS was no more tightly bound than CHOR in our MD simulations. Electrostatic interactions between EcCM and CHOR are similar to those between EcCM and TS. Three hydrophobic interactions between EcCM and CHOR are all absent in EcCM·TS, presumably because of the more polar character and the more contracted geometry of TS than CHOR (Fig. 5). The simulation of EcCM·CHOR showed that the active site of EcCM is extremely proficient in inducing the substrate to form a catalytically competent structure (NAC). By analyzing the conformers of bound substrates, the following mechanism of NAC formation is proposed. (*i*) The two salt bridges between carboxylates of CHOR and Arg-11* and Arg-28 position the reactive terminus (C16) tucked under Val-35. (*ii*) The van der Waals contact of C16 with Val-35 efficiently constrains the space between reactive termini (C16 and C5), resulting in a shorter C5-C16 distance without showing any correlation between the distance of Val-35(CG1) to C16 and the distance of C5 to C16. We concluded that the $>10^6$ catalytic prowess of EcCM originates from the conformational restriction of GS structure to resemble NAC structure, resulting in ≈70% of NAC population in the EcCM active sites.

We are grateful to Drs. Kalju Kahn and Edmond Lau for assistance and helpful discussion throughout the project. The authors gratefully acknowledge computer time on the Univ. of California (Santa Barbara) SGI Origin2000 and at the National Partnership for Advanced Computational Infrastructure (San Diego Supercomputer Center). S.H. was supported by a fellowship from Ewha Woman's University and is presently supported by National Science Foundation Grant MCB-9727937.

1. Pauling, L. (1946) *Chem. Eng. News* **24,** 1375–1377.
2. Ganem, B. (1996) *Angew. Chem. Int. Ed. Engl.* **35,** 937–945.
3. Lee, A. Y., Stewart, J. D., Clardy, J. & Ganem, B. (1995) *Chem. Biol.* **2,** 195–203.
4. Chook, Y. M., Gray, J. V., Ke, H. M. & Lipscomb, W. N. (1994) *J. Mol. Biol.* **240,** 476–500.
5. Sogo, S. G., Widlanski, T. S., Hoare, J. H., Grimshaw, C. E., Berchtold, G. A. & Knowles, J. R. (1984) *J. Am. Chem. Soc.* **106,** 2701–2703.
6. Addadi, L., Jaffe, E. K. & Knowles, J. R. (1983) *Biochemistry* **22,** 4494–4501.
7. Bruice, T. C. (2002) *Acc. Chem. Res.*, in press.
8. Andrews, P. R., Smith, G. D. & Young, I. G. (1973) *Biochemistry* **12,** 3492–3498.
9. Lee, A. Y., Karplus, P. A., Ganem, B. & Clardy, J. (1995) *J. Am. Chem. Soc.* **117,** 3627–3628.
10. Xue, Y. F., Lipscomb, W. N., Graf, R., Schnappauf, G. & Braus, G. (1994) *Proc. Natl. Acad. Sci. USA* **91,** 10814–10818.
11. Kast, P., Hartgerink, J. D., Asifullah, M. & Hilvert, D. (1996) *J. Am. Chem. Soc.* **118,** 3069–3070.
12. Mattei, P., Kast, P. & Hilvert, D. (1999) *Eur. J. Biochem.* **261,** 25–32.
13. Gustin, D. J., Mattei, P., Kast, P., Wiest, O., Lee, L., Cleland, W. W. & Hilvert, D. (1999) *J. Am. Chem. Soc.* **121,** 1756–1757.
14. Guilford, W. J., Copley, S. D. & Knowles, J. R. (1987) *J. Am. Chem. Soc.* **109,** 5013–5019.
15. Wiest, O. & Houk, K. N. (1995) *J. Am. Chem. Soc.* **117,** 11628–11639.
16. Xue, Y. F. & Lipscomb, W. N. (1994) *J. Mol. Biol.* **241,** 273–274.
17. Liu, D. R., Cload, S. T., Pastor, R. M. & Schultz, P. G. (1996) *J. Am. Chem. Soc.* **118,** 1789–1790.
18. Wiest, O. & Houk, K. N. (1994) *J. Org. Chem.* **59,** 7582–7584.
19. Worthington, S. E., Roitberg, A. E. & Krauss, M. (2001) *J. Phys. Chem. B* **105,** 7087–7095.
20. Bartlett, P. A., Nakagawa, Y., Johnson, C. R., Reich, S. H. & Luis, A. (1988) *J. Org. Chem.* **53,** 395–3210.
21. Pawlak, J. L., Padykula, R. E., Kronis, J. D., Aleksejczyk, R. A. & Berchtold, G. A. (1989) *J. Am. Chem. Soc.* **111,** 3374–3381.
22. Guo, H., Cui, Q., Lipscomb, W. N. & Karplus, M. (2001) *Proc. Natl. Acad. Sci. USA* **98,** 9032–9037.
23. Khanjin, N. A., Snyder, J. P. & Menger, F. M. (1999) *J. Am. Chem. Soc.* **121,** 11831–11846.
24. Campbell, A. P., Tarasow, T. M., Massefski, W., Wright, P. E. & Hilvert, D. (1993) *Proc. Natl. Acad. Sci. USA* **90,** 8663–8667.
25. Gray, J. V. & Knowles, J. R. (1994) *Biochemistry* **33,** 9953–9959.
26. Lyne, P. D., Mulholland, A. J. & Richards, W. G. (1995) *J. Am. Chem. Soc.* **117,** 11345–11350.
27. Davidson, M. M., Gould, I. R. & Hillier, I. H. (1996) *J. Chem. Soc. Perkin Trans.* **1,** 525–532.